Chapter 5

Pulse Electroplating of Ultrafine Grained Tin Coating

Ashutosh Sharma, Siddhartha Das and Karabi Das

Additional information is available at the end of the chapter

http://dx.doi.org/10.5772/61255

Abstract

In the electronic packaging industries, soldering materials are essential in joining various microelectronic networks. Solders assure the reliability of joints and protect the microelectronic packaging devices. They provide electrical, thermal, and mechanical continuity among various interconnections in an electronic device. The service performance of all the electronic appliances depends on high strength and durable soldering materials. Lead-containing solders are in use for years, resulting in an extensive database for the reliability of these materials. However, due to toxicity and legislations, lead-free solders are now being developed. As tin (Sn) is the major component of solders, this chapter presents the detailed results and discussion about the metallurgical overview of Sn, synthesis, and characterization of pulse electrodeposited pure tin finish from different aqueous solution baths. The experiments on pulse electrodeposition such as common tin plating baths employed, their chemical compositions, rationale behind their selection and their characterization by bath conductivity and cathodic current efficiency, microstructures, and tin whisker growth are discussed. Further, the effect of pulse electrodeposition parameters such as current density, additive concentration, pH, duty cycle, frequency, temperature, and stirring speed on microstructural characteristics of the coating obtained from sulfate bath and their effect on grain size distribution have been presented.

Keywords: Tin plating, pulse electrodeposition, morphology, plating baths, grain size

1. Introduction

1.1. Background

Lead-bearing solders are in use till date due to their indispensable properties [1–3]. Firstly, it is very cheap, available in abundance and provides good physical and chemical bonding to the substrate without interfering with the substrate [4–5]. Secondly, lead (Pb) reduces the surface tension of pure tin, which is 550 mN/m at 232°C, and the lower surface tension of 63Sn-37Pb solder (470 mN/m at 280°C) facilitates wetting [4, 6, 7]. The presence of Pb also helps

to prevent the white tin (β-Sn) to gray tin (α-Sn) allotropic phase transformation from occurring in high-Sn solders upon cooling below 13ºC [7]. This makes it a prime choice for soldering.

1.2. Replacement of Pb

There are many technology-based problems that can serve as reasons for the elimination of Sn-Pb solders. First, it has been already proved in the past that many lead-free candidate solders exhibit significantly better strength and fatigue life properties [4, 6]. Secondly, Pb and Pb compounds have been cited by the Environmental Protection Agency (EPA) as one of the top 17 chemicals posing the greatest threat to human life and the environment [7, 8]. In view of these reasons, elimination of Pb from electronics is necessary in electronics packaging [1, 6].

1.3. The lead-free definition and regulations

Legislations to restrict the use of Pb were first implemented in the USA in 1991 with the Lead Exposure Reduction Act of 1991 and the Lead Exposure Act of 1992, which bans Pb in some applications and limits Pb content in others to less than 0.1% [7, 8]. In the United States, the National Electronics Manufacturing Initiative (NEMI) program was developed to research on lead-free alternatives [9]. In Japan, this movement is connected to the Lead-free Soldering Research Council (1994 to 2000) within the Japan Institute of Electronic Packaging. Japan Electronics and Information Technology Industries Association (JEITA) has set guidelines for lead-free products, which was published in 1999 [10, 11]. These companies aimed to use lead-free solders in mass-produced consumer products and to implement lead-free soldering technologies in their products by 2003 [2]. In Europe, the EU directives (WEEE) and (RoHS) have issued a ban on the use of lead in consumer goods [12, 13].

2. Metallurgical overview of Sn

Pure Sn has two allotropes, white tin (β-Sn, metallic) and gray tin (α-Sn, semiconductor). The most common form of Sn in real life is white tin, which transforms to gray tin at temperatures below 13ºC [14]. β-Sn possesses body-centered tetragonal crystal structure with lattice parameters $a = b = 0.5820$ nm and $c = 0.3175$ nm [15]. This c/a ratio of 0.546 gives rise to highly anisotropic behavior in Sn. The mechanical properties are very poor, the hardness being 11 Hv and tensile strength 44 MPa [16]. This is largely due to its lower melting point relative to common engineering metals such as aluminum (Al), copper (Cu), and steel [14–16].

2.1. Pb-free Sn alloys

A relatively large number of Pb-free solder alloys have thus been proposed so far, Sn being the primary or major constituent. The two other elements that are major constituents are indium (In) and bismuth (Bi). Other alloying elements are zinc (Zn), silver (Ag), antimony (Sb), copper (Cu), and magnesium (Mg), and in one case, a minor amount of Pb [1–3]. The most popular Pb-free alloy system candidates are listed in a thorough review paper

by Abtew and Selvaduray [1]. The most important characteristics that must be considered in selecting suitable Pb-free solder candidates are: nontoxic; availability; sufficient electrical as well as thermal conductivity; adequate mechanical properties compatible with metallic substrates such as Cu, nickel (Ni), Ag, or gold (Au); economically viable; acceptable melting and processing temperatures; and less temperature effects on substrates, printed circuit boards(PCBs), etc. [1–4, 6].

2.2. Intermetallic compounds and whisker growth

Due to the Pb-free solder implementation, pure Sn and Sn-Cu, Sn-Ag are commonly used to replace eutectic Sn-Pb as the surface finish on the lead-frames and metal terminations of passive devices [17, 18, 19]. However, in Sn-rich lead-free finish, Sn whiskers have been found to form, which poses a serious threat for the reliability of passive devices. The Sn whisker formation was first reported in 1946 [20]. It is generally accepted that the driving forces of Sn whiskers mainly attribute to the internal stresses, the dissolution of the metal under-layer, and the interfacial compound formation. There are two intermetallic compounds of Cu and Sn below 300ºC, they are Cu_6Sn_5 and Cu_3Sn. The Cu_6Sn_5 forms at room temperature while Cu_3Sn forms after annealing at elevated temperatures [21, 22]. Some intermetallic compounds (IMCs), such as AuSn4 for Sn/Au couples, Cu_6Sn_5 for Sn/Cu couples, and Ni_3Sn_4 for Sn/Ni couples, even form at room temperature [23, 24].

Based on these three main root-causes of Sn whisker formation, three methods are devised by researchers to retard the Sn whiskers formation: (1) choosing optimal thickness of the finish layer, (2) alloying with other metal elements, and (3) adding a reaction barrier layer beneath the finish layer [25–27].

3. Synthesis routes and technologies for solder fabrication

There are many synthesis routes for the fabrication of solders varying from solid state mechanical alloying, powder metallurgy, sol gel, melting and casting route, chemical routes, gaseous phase sputtering or evaporation methods, electrodeposition method, etc. [28-35]. Among all these methods, we will discuss techniques related to thin film pulse electrodeposition of solders. The other methods are not discussed here because they are out of the scope of this chapter.

3.1. Electrodeposition

Both evaporation and sputter deposition techniques require high vacuum and/or high temperature processing, which increases operation costs and cause inter-diffusion problems. Compared to these fabrication processes, electrodeposition is an economically viable process [36]. It can be used to plate either single layer or multilayer deposits with easy and precise control of the thickness and composition of each layer. Electrodeposition can be performed on substrates with varying sizes and complex shapes and the deposit can be very thin or very thick [37–38]. There are, however, safety and environmental concerns related with chemical

treatment and safe disposal of wastes. Numerous metals and metal alloys have been successfully electrodeposited from aqueous solutions. The most useful electrodeposited metals include Sn, Cr, Cu, Ni, Ag, Au, Zn, and alloys such as chromium-nickel (Cr-Ni), iron-cobalt (Fe-Co), and various Sn alloys [36–38].

3.2. General aspects of electrodeposition

In electrodeposition, metal ions present in a solution, the electrolyte, are reduced at the surface of an electrode to form a metal layer, as shown in Fig. 1.

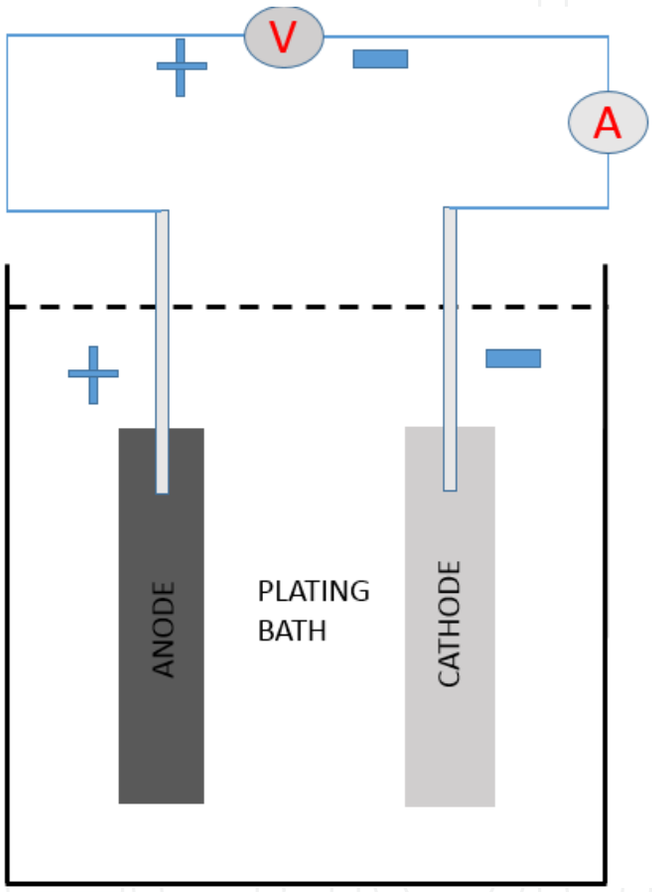

Figure 1. A schematic for the electrodeposition process.

This process essentially consists of: (1) an anode (the positive electrode), (2) a cathode (the item to be electroplated, which is the negative electrode), (3) the electrolyte acts as a transport medium for the tin ions to be deposited at the cathode as a coating on the item to be electroplated, (4) an electric current or voltage source for controlling the deposition, and (5) various peripherals for contacting the electrodes, stirring and heating the solution, etc. [36–37].

In electrodeposition, the metal is deposited over a conductive substrate by the application of electric current through the electrolytic bath. The current provides sufficient energy to proceed the oxidation-reduction reactions at anode and cathode, respectively. The metal ions in the

http://dx.doi.org/10.5772/61255

electrolyte accept the electrons and get deposited on the substrate. The weight of the deposited material can be calculated from the relation given by Faraday's laws [37–39]:

$$\frac{\text{Thickness}}{\text{time}} = \frac{J(ECE)(CCE)}{\text{density}} \tag{1}$$

where thickness of the deposit is in mg, time in seconds, J = current density, ECE = electrochemical equivalent, CCE = current efficiency (ratio of actual/theoretical weight deposited), and density of deposit is in g/cm^3.

3.3. Cathodic and anodic reactions

Electrochemical deposition of metals and alloys involves the reduction of metal ions from aqueous, organic, and fused-salt electrolytes. In this thesis, electrodeposition from aqueous solutions is being considered. The reduction of metal ions M^{n+} in aqueous solution is represented by [37–39]:

$$M^{n+} + ne^- \rightarrow M \tag{2}$$

Reaction (2) is often accompanied by hydrogen evolution. In acid solutions, we have:

$$2H^+ + 2e^- \rightarrow H_2 \tag{3}$$

In neutral and basic solutions, hydrogen evolution follows the equation:

$$2H_2O + 2e^- \rightarrow H_2 + 2OH^- \tag{4}$$

At the anode, the anodic reactions are as follows. In an acidic solution, we have:

$$2H_2O \rightarrow O_2 + 4H^+ + 4e^- \tag{5}$$

In an alkaline solution, the anode reaction is:

$$4OH^- \rightarrow O_2 + 2H_2O + 4e^- \tag{6}$$

For a soluble anode, oxidation reactions, which will dissolve the anode into solution:

$$M \rightarrow M^{n+} + ne^- \tag{7}$$

The equilibrium electrode potential between a metal and a solution of its ions is given by the Nernst equation:

$$E_{M/M^{n+}} = E^{o} + \frac{RT}{nF} \ln C_{M^{n+}} \tag{8}$$

where E^{o} is the standard electrode potential, R is the gas constant, F is the Faradaic constant, and $C_{M^{n+}}$ is the metal ion concentration. It can be noticed that the value of $E_{M/M^{n+}}$ depends on the concentration of metal ions to be plated, addition of additives, current density, etc. [38, 39].

3.4. Electrolyte conductivity

The conductivity of an electrolyte depends on the degree of dissociation, the mobility of individual ions, temperature (and thus viscosity), and the electrolyte composition. In aqueous solutions, the ionic conduction depends on the degree of dissociation of dissolved species in the solution [38, 39]. In order to increase the conductivity of electrolytes, certain salts and acids or alkali are added; these are known as supporting electrolytes. For acid electrolytes, chlorides and acids are useful; for neutral electrolytes, chlorides are useful; and for alkaline electrolytes, sodium hydroxide or cyanides are useful [39]. Generally, a marked decrease in conductivity at higher concentration is due to the greater coulombic forces acting between the ever closer ions in solution. This leads to the loose association of opposite charged ions that are effectively neutral and thus no longer contribute to the overall conductivity [39].

3.5. Polarization and overpotential

The equilibrium potential of an electrode differs in an electrochemical cell after the application of current. Suppose the equilibrium potential of an electrode when there is no external current flowing is E. After the application of an external current (I), the potential of the electrode change by E(I), the overpotential (η) can be given as:

$$\eta = \mathrm{E}(\mathrm{I}) - \mathrm{E} \tag{9}$$

It can be also expressed as in terms of current and voltage by the Tafel equation:

$$\eta = \mathrm{a} + \mathrm{b} \log \mathrm{I} \tag{10}$$

where a and b are constants.

The overpotential η is required to overcome hindrance of the overall electrode reaction, which is usually composed of a sequence of partial reactions, charge transfer, diffusion, chemical reaction, and crystallization [36, 38]. The overpotential is generally used as a measure of the extent of polarization. Polarization demonstrates departure of the electrode potential from the

http://dx.doi.org/10.5772/61255

equilibrium value upon passage of a Faradaic current [39]. Depending upon the nature and sites of the inhibition factors, there may be different kinds of overpotentials, such as charge transfer overpotential or activation overpotential, which is caused by inhibition of the charge transfer taking place across the close proximity of solution/cathode interface.

Thus, four different kinds of overpotential are distinguished and the total overpotential η can be considered to be composed of four components: where η_{ct}, η_d, η_r, and η_c are, as defined above, charge-transfer, diffusion, reaction, and crystallization overpotentials, respectively. The electrode reaction can then be represented by a resistance (R_E), composed of a series of resistances (or more precisely, impedance), which represent the different steps: R_{mt}, R_{ct}, and R_{rxn}. A fast reaction step is characterized by a small resistance, while a slow reaction step is represented by a high resistance. In other words, R_E will be the sum of all the resistances Rmt, R_{ct}, and $R_{rxn,}$ as shown in Fig. 2 [38].

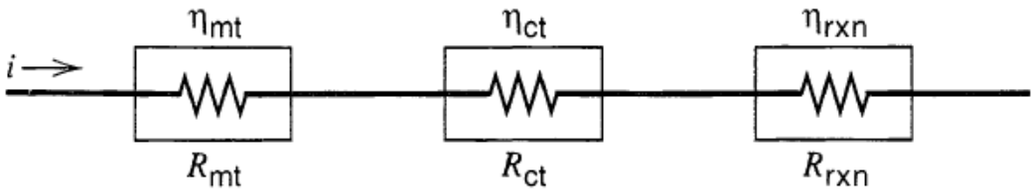

Figure 2. Processes in an electrode reaction represented as resistances (From A.J. Bard, and L.R. Faulkner, Chapter 1: Introduction and Overview of Electrode Processes, Page 24, Electrochemical Methods - Fundamentals and Applications, 2nd Edition. Reprinted by permission of John Wiley & Sons, Inc. Copyright 2001 © John Wiley & Sons, Inc.

3.6. Pulse current electrodeposition

In olden times, direct current (DC) electrodeposition had only one parameter, namely, current density that is variable. In modern times, pulsed current (PC) plating where the potential or current density alternates rapidly between two different values is used [36–39]. This is accomplished with a series of pulses of equal amplitude, duration, and polarity, separated by a period of zero current, and time (t) axis as shown in Fig. 3. Each pulse consists of an on-time (T_{on}), during which potential and current is applied, and an off-time (T_{off}), during which open circuit potential and zero current is applied.

The duty cycle is given by the equation:

$$\text{Duty Cycle } (\%) = \frac{T_{on}}{T_{on} + T_{off}} \tag{11}$$

The average current density is defined as:

$$J_{average} = (J_{peak}) \times \text{ Duty Cycle} \tag{12}$$

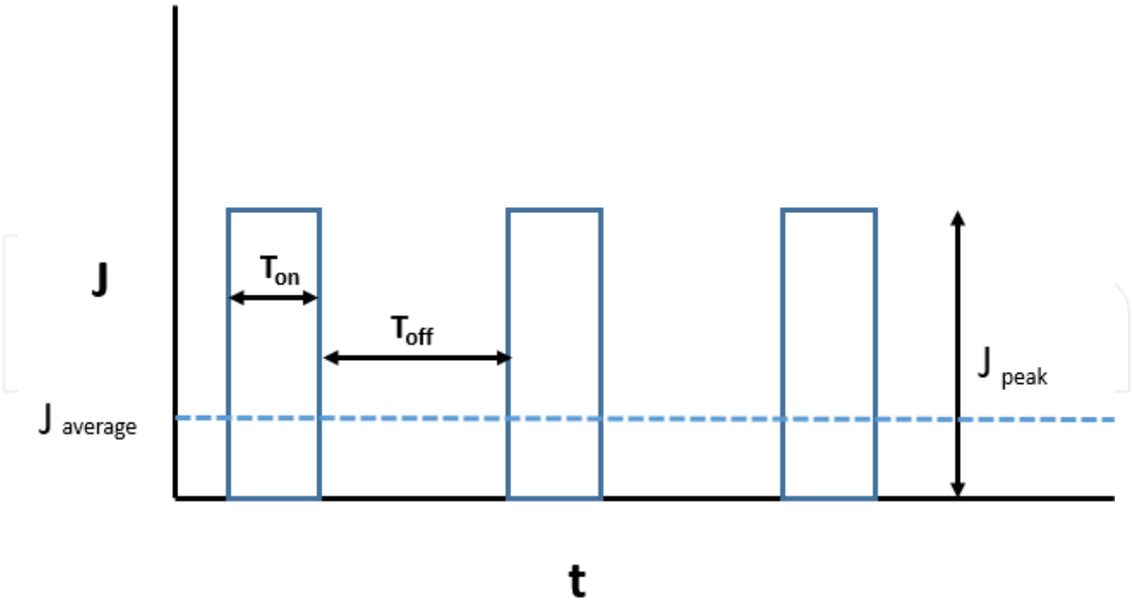

Figure 3. Schematic diagram of pulsed current waveform.

$J_{average}$ is the average current density and J_{peak} is the peak current density [35, 39, 40]. The average current density in PC plating is similar to the current density used in DC plating. For a given average current density, a number of combinations of different peak current densities and on-off times are available. This gives PC plating two important features. Firstly, a very high instantaneous current density, one to two orders in magnitude greater than the steady-state limiting current density as reported, can be used without depleting the metal ions at the electrode surface [40]. This favors the initiation of the nucleation process and greatly increases the number of grains per unit area, resulting in a finer grained deposit with better properties than conventional DC plating. Secondly, during the off-time period, adsorption and desorption, as well as recrystallization of the deposit occurs, which can control the microstructure of the deposits [36, 40, 41].

4. Electrodeposition of Sn

Sn can be electrodeposited from both acidic and alkaline aqueous solutions [42, 43]. In acidic baths, Sn usually exists as Sn^{2+} ions, while in alkaline baths, Sn^{4+} is the more stable species. The various Sn plating baths available in literature are discussed below.

4.1. Sodium stannate baths

The alkaline stannate electrolytes usually contain sodium or potassium stannate and the corresponding alkali metal hydroxide. These electrolytes are environment friendly, as they are non-corrosive in nature and do not require other organic additives [42, 43]. The alkaline tin baths have a very high throwing power and can be operated over a wide current density range.

The tin coatings electroplated from alkaline electrolytes possess improved solderability, since they do not require any organic additive agents [44, 45]. This leads to a great improvement in wettability. One major disadvantage of alkaline plating baths is that highly alkaline baths may dissolve the photoresist used to define areas on semiconductor wafers. Alkaline plating baths also usually require higher plating temperatures (60–70°C) as compared to acidic ones [46].

4.2. Stannous sulfate baths

Sulfate baths are primarily used for bright acid Sn plating. Organic agents are necessary if bright and dense films are to be obtained. Electroplating of tin from acidic stannous (divalent Sn) solutions consumes less electricity than alkali stannate solutions (tetravalent Sn) [42–45]. The major drawback of this system is Sn oxidation. At high current density, soluble Sn anodes are passivated due to the formation of SnO_2. Irregular, dendritic, needle-like electrodeposits of tin are in general obtained from acidic electrolytes without organic additives [47–49]. To improve the surface finish, morphology, and adhesion during acidic tin plating, various organic chemicals as additives have been investigated in the past [50–52]. In the literature, we observe that sulfate baths have been used widely to plate pure Sn and various Sn alloys in electronics industries [53].

4.3. Stannous chloride baths

For tin electroplating, sulfate baths use a number of additives to produce a homogeneous deposit [47–53]. However, in-spite of these advantages, the use of additives is undesirable for health concerns. Moreover, adverse effects on plating efficiency and the working environment have been observed [54, 55]. In case of alkaline baths, the same is true as it requires heating the solution that causes bubble formation [44–46]. Also tin is tetravent in alkaline baths causing more power. In view of these disadvantages, recently, He *et al*. developed a bath containing citric acid or its salt and an ammonium salt [53]. In the same line, Sharma *et al*. produced bulk tin films from stannous chloride-citrate bath and found improved thermal and mechanical properties [56].

4.4. Methanesulfonic acid baths

The problem of oxidation of Sn^{2+} to Sn^{4+} can be minimized by using a reducing acid Methanesulfonic acid (MSA) bath as compared to sulfate bath. MSA is much less corrosive to electronic materials than sulfuric acid [55]. It forms a clear solution, have high dissolving power and less sensitive to Sn oxidation at higher current densities [57]. Different combinations of methanesulfonate baths have been developed to electrodeposit both pure Sn and various Sn alloys by adding different additives [58].

4.5. Pyrophosphate baths

There are a number of pyrophosphate baths available in the literature [42]. These types of baths containing $P_2O_2^{2-}$ is considered as one of the most stable systems and is widely used for Sn plating [59, 60]. However, its use is limited in literature due to one disadvantage, that it requires

more control and maintenance than the other plating baths. The operational temperature should not exceed 43–60°C because the pyrophosphate complex hydrolyzes to orthophosphate at temperatures higher than 60°C, which degrades the solution [42, 61].

5. Electrodeposition of Sn alloys

According to the electrochemical series of metals, we know that the reduction potential of two elements would be different [35]. For a solution containing two or more different metal ions at low overpotential, the metal with the most noble reduction potential will deposit at a faster rate [35, 36]. If the electrode potential difference is far apart, then metal alloy electrodeposition may be impossible. The difference can be eliminated in view of the Nernst equation by modifying the activity values and feasibility of the co-deposition can thus be determined [37, 39]. This can be achieved by inducing a considerable change in ionic concentrations via complex ion using certain complexing agents. In the past, thiourea has been utilized as a complexing agent for the electrodeposition of Sn-Ag and Sn-Ag-Cu alloys [62, 63]. The formation of complexes by bonding the metal ions with complexing agents will decrease the concentration of the free metal ions in the solution significantly and modify the reduction potential of the metal ions [64, 65]. With an increase in overpotential, the electrodeposition reaction will progress from the charge transfer region to the mix and then to the mass-transfer regime. Under mass transfer control at sufficiently higher overpotentials, the relative deposition rates of two or more metals will be governed by the concentrations and the diffusion coefficients of the metal ions [38, 39]. For alloy deposition, the basic mechanism remains the same as the Sn deposition discussed in the previous section. The summary of the previous studies on different types of plating baths are given in Table 1.

Coating	Processing Methods	Plating bath	Applications	Reference
Sn	Electroplating	Sodium stannate bath + halides	Lead-free	Abdel Rahim *et.al*., 1986 [44]
Sn	Electroplating	Sodium stannate bath + sorbitol	Soldering	Broggi *et al*., 2003 [45]
Sn	Pulse electroplating	Sodium stannate bath	Lead-free	Sharma *et al*., 2012 [46]
Sn-Co	Electroplating	Stannous sulfate Gluconate bath	Lead-free	Rehim *et al*., 1996 [48]
Sn	Electroplating	Stannous sulfate bath + aldehydes	Solder joints	Tzeng *et al*., 1996 [49]
Sn	Electroplating	Stannous sulfate bath + Benzal acetone and N,N-bis(tetraoxyethylene)octadecylamine	Lead-free	Nakamura *et al*., 1997 [50]

http://dx.doi.org/10.5772/61255

Coating	Processing Methods	Plating bath	Applications	Reference
Sn-Cu, Sn-Bi, and Sn-Ag-Cu	Electroplating	Stannous sulfate bath + polyoxyethylene laurylether	Lead-free	Fukuda *et al*., 2003 [51]
Sn-Co	Electroplating	Stannous sulfate bath + DS-10 synthanol, coumarin, formalin (37% solution)	Flip Chip technology	Medvedev *et al*., 2001 [52]
Sn	Pulse electroplating	Stannous sulfate bath + triton X 100	Solder joints	Sharma *et al*., 2013 [54]
Sn	Pulse electroplating	Stannous chloride bath	Wafer bumps	He et al., 2008 [53]
Sn	Pulse electroplating	Stannous chloride bath	Lead-free	Sharma *et al*., 2013 [56]
Sn	Electroplating	MSA bath + PEG, PPG+ Phenolphthalein	Solder bumps	Martyak *et al*., 2004 [57]
Sn	Electroplating	MSA bath + per-fluorinated cationic surfactant	Solders	Low *et al*., 2008 [58]
Sn	Electroplating	Pyrophosphate bath + dextrin+ gelatin	Solders	Vaid *et al*., 1957 [60]
Sn	Electroplating	Pyrophosphate bath + gelatin	Li-ion battery	Kim *et al*., 2010 [59]
Sn-Ag and Sn-Ag-Cu	Electroplating	Stannous sulfate bath +thiourea	Solders	Ozga *et al*., 2006 [62]
Sn-Ag-Cu	Electroplating	Stannous sulfate bath +thiourea+ polyoxyethylene laurylether	Lead-free	Fukuda *et al*., 2002 [63]
Sn-Zn	Electroplating	Stannous chloride bath + PEG	Lead-free	Lin *et al*., 2003 [64]
Ni, Sn, and Ni-Sn	Electroplating	Pyrophosphate-glycine bath	Lead-free	Lacnjevac *et al*., 2012 [65]

Table 1. Summary of various studies on electrodeposition of Sn.

6. Process parameters and nanostructure formation

The electrodeposition method is dependent on several processing parameters involved in the electrodeposition process. Therefore, to obtain the desired properties, it is essential to optimize

the operating parameters. The effect of these parameters on tin electrodeposition is discussed in the following sections.

6.1. Current density

The current density is the primary controlling parameter in pulse electrodeposition. The average current density $J_{average}$, is given by peak current density J_{peak} x Duty Cycle. This enables us to achieve a very high current density in pulse electrolysis without depleting the metal ions at the electrode surface [66]. A high overpotential associated with higher pulse current density raises the nucleation rate resulting in fine grained deposit and thus improved properties can be obtained [38–40]. For a stable growth, the critical radius of the electrodeposited nucleus varies inversely to the cathodic overpotential. The higher the cathodic overpotential, the higher the nucleation rate will be and vice versa [66, 67]. Thus, the grain size decrease with the increase in cathodic overpotential and finer grains are obtained. A higher current density also leads to the development of dendritic morphology of the deposits [49–54, 56]. The dendritic morphology can be suppressed by using additives. For alloy deposition, the change in alloy morphology has been noted by several researchers with increase in current densities [64, 65, 68].

The dendritic or irregular shaped morphology in response to the current density is due to the fact that if there is a significant increase in the current density, it increases the nucleation rate and is also associated with a higher rate of hydrogen evolution. Due to high overpotential at this state, the rate of diffusion of Sn2+ ions towards cathode becomes significant over its replenishment from the electrolyte [68, 69]. This phenomenon creates a concentration gradient in the vicinity of electrolyte/cathode interface. As a consequence, the deposition occurs preferentially on certain protrusions (heterogeneous active sites on the cathode in a random manner. This type of non-uniform growth kinetics has also been observed in copper plating [70]. The cathodic current efficiency at this stage is poor indicating a rapid hydrogen evolution which decreases the concentration of Sn2+ ions in the electrolyte.

6.2. pH

The effect of pH in tin plating has not been discussed in detail in the literature. The majority of the tin plating baths available in literature are acidic in nature. As a general statement the rate of deposition increases with pH [71]. Bath pH not only affects the deposition rate but modifies the crystal orientation. Some people have noted a pH induced texture in Sn grains from acidic electrolyte [72]. Ebrahimi *et al*. investigated the effect of pH on nickel deposits [73]. He found that the pH values of 4.5, 4.7, and 5.0 resulted in grain size of 79, 45, and 56 nm, respectively. The increasing pH value from 2.8 to 5.1 enhanced the nucleation rate of nickel crystals, which corresponded to decreasing grain size from 343 to 35 nm. For copper electrodeposition, Natter and Hempelmann reported the smallest copper grain size of 8 nm at pH 1.5–2.0 and a continuous increase of the grain size up to 100 nm at pH 11.5 [74]. The morphology of the deposited Sn coatings with different bath pH gets refined with an increase in pH. At a high value of pH around 2, irregular and porous deposits are observed due to the progressive increase in hydrogen evolution reaction. However, at a very high pH (=3), the deposits turn powdery due to severe hydrogen gas evolution [54].

http://dx.doi.org/10.5772/61255

6.3. Temperature

The majority of acid type formulations operate at room temperature, while alkaline tin baths need to be heated at higher optimum temperatures. As the temperature increases, the rate of deposition also increases [41, 54, 74]. The velocity (diffusion and migration) of the metal ions and inhibitor molecules are functions of the temperature. The viscosity of the electrolyte decreases at high temperature, therefore, the diffusion rate and the velocity of metal ions and inhibitor molecules are increased. Sahaym *et al*. studied the effect of bath temperature in Sn electrodeposits and found the pyramid type morphology at elevated temperatures [75]. They varied the bath temperature from 35ºC to 85ºC and explained that at higher bath/substrate temperature, the cooling rate of the adatoms will be slower. This indicates that at higher plating temperatures, adatoms can travel to longer diffusion distances on the cathode. This shows that an increase in the bath temperature may lead to increased grain growth and a smooth coating surface. Similar results are shown by Sharma *et al*. [74]. Bath temperature has been also shown to affect the morphology of the whiskers that formed upon aging at room temperature [75]. The metal ions and the inhibiting species have a higher mobility at high temperatures. It results in an increase in the concentration of metal ions towards the cathode and a decreases in the cathodic overpotential is observed. This increases the energy barrier (ΔG) for the nucleation process according to the equation given by Glasstone in reference [74], resulting in coarser grain size at higher temperature:

$$\Delta G \propto \left\{ \frac{1}{\left(\eta + \left[\frac{C'}{C} \right] \right)^2} \right\} \tag{13}$$

where C' is the activity of the Sn^{2+} on the electrode and C is the activity of Sn^{2+} in the bulk solution. The adsorption rate of inhibiting species decreases at high temperatures due to the decrease in viscosity causing an enhanced grain growth. It is reported in the past that in an acidic plating bath may decompose at high temperature [41, 42]. Therefore, the plating bath color may also change from light to dark yellow and get precipitated. This may be due to the decomposition of the sulfate entity or oxidation of Sn^{2+} to Sn^{4+}, which affects the solution chemistry [41–42, 45, 46]. The plating bath decomposition at elevated temperatures will decrease the bath conductivity and hence the current efficiency decreases beyond 40°C, with a negligible change in deposit morphology.

6.4. Additives

Although literature review about composite films and nanocrystalline films contains information about additives, additives for conventional metal deposition are still important as those additives would provide another aspect of information about deposition mechanism and novel additives. Popular organic additives that have been used in electrodeposition are gelatin,

thiourea, EDTA (Ethylenediaminetetracetic acid), citric acid, benzotriazole (BTA), and inorganic additives such as chloride, are covered in this chapter. Nakamura *et al*. used various organic additives such as benzalacetone (BA) and N, N-bis (tetraoxyethylene) octadecylamine [50]. They found that by increasing the concentration of BA, smaller grains are obtained and roughness increases. Further, when both are used with a high concentration of BA, fine-grained deposits are obtained due to a synergistic action of these adsorbed species. Tzeng *et al*. studied the behavior of aliphatic and aromatic aldehyde groups in tin electrodeposition. They found that as compared to formaldehayde and propionoaldehyde, benzaldehyde is hydrophobic in nature showing more overpotential and thus acts as the best grain refiner [49]. Surface active agents such as Triton X-100, aromatic carbonyl compounds, amine-aldehyde reaction products, methane sulphonic acid and its derivatives, etc. [50, 52, 57, 58, 76, 77], are added to plating baths. The addition of excessive amounts of additives, high current density, and an increase in the concentration of metal ions in the electrolyte may affect the deposit solderability. It is mainly attributed to the oxidation of tin ions in the solution, as well as the aging of the deposit in the presence of organic brighteners [76–78]. Fine-grained and smooth deposits were obtained from acid stannous sulphate solutions containing some aromatic ketones [50]. It was found that these organic compounds were adsorbed on the cathode surface and enhanced the overpotential. In acidic solutions, many other chemicals, such as polyoxyethylene laurylether, triethanolamine, sorbitol, sodium gluconate, 1, 4- hydroxybenzene, Trion X-100, or polypropylene glycol may be added as complexing agents. The additives are necessary to improve solution stability and deposit morphology. However, an excessive amount of additives would make the coating less solderable [54, 57, 58, 78].

For alkaline stannate bath additives, few reports are available in literature. They usually do not require any additives since deposition occurs at a very negative potential and hydrogen evolution runs parallel with tin deposition acting as a leveler. However, the disadvantage is the diffusion of hydrogen inside the tin deposits [74–79]. In literature, the effect of additives has not been discussed in detail for chlorides electrolytes. Sekar *et al*. investigated the effect of additives in detail on pulse elctrodeposition of tin containing Gelatin, β-naphthol, polyethylene glycol, peptone, and histidine as additives [80]. They observed a grain refinement brought about by additives but a marked decrease in current efficiency and found that the bath containing peptone has the lowest crystallite size with better corrosion properties. The selection of organic additive(s) generally depends upon the nature of the metal ions, bath pH, as well as the temperature of the plating solution/substrate. For instance, semi-bright or bright nickel plating solution has different sets of additives as compared to the additives used in acidic zinc plating. Similarly, additives used in acid tin plating baths are different than those used in alkaline tin plating. However, the coating morphologies and properties obtained from acidic and alkaline solutions may or may not be similar to each other. In MSA baths, glycol type additives, PEG, PPG, and Phenolphthalein have been tried in literature [55]. Glycol-type additives are effective in minimizing hydrogen gas evolution at low overpotentials and refining the grain structure across a wide current density range. These additives are active in the presence of Phenolphthalein [57]. Low and Walsh used the perfluorinated surfactant in MSA bath and observed that the adsorption of the surfactant hindered hydrogen evolution and reduced the peak and limiting current densities [58]. There is little information on

pyrophosphate baths in literature. Pyrophosphate baths include mostly glycol additives used in SnAg type solder bumps. These baths require more control of the electrodeposition parameters. Normally chelating agents and organic additives such as triethanolamine, sodium gluconate, 1, 4-hydroxybenzene, and Triton X-100 have been added in pyrophosphate baths [42, 59, 60, 61, 81, 82]. The additives are active only up to a certain concentration and have a beneficial effect on the microstructure of the deposits by increasing the cathodic polarization.

At higher concentration of additives, the progressive evolution of hydrogen gas leads to the development of non-uniform powdery deposits. The powdery deposits generally arise due to the adsorption and absorption of the hydrogen gases in the deposits according to the following reactions [54, 83]:

$$2H_{ads} \text{---} H_2 \tag{14}$$

$$H^+ + e^- \text{----} H_{ads} \tag{15}$$

$$H_{ads} \text{----} H_{abs} \tag{16}$$

The additive blocks the association of generated hydrogen atoms according to Equation (14). Consequently, the concentrations of H_{ads} rises following Equation (15). The combined effect of these two phenomena (Equations 15 and 16) results in absorption of hydrogen atoms in the deposits according to Equation (16).

6.5. Duty cycle and frequency

The pulse deposition rate is given by the pulse current density and other parameters such as 'on' time (T_{on}) and 'off' (T_{off}) time. The pulse length T_{on} and T_{off} time have significant effect on grain size. An increase in pulse current density at constant length T_{on} and constant average current density with an increase in T_{off} time cause an increase in grain-size, because grain growth takes place during the T_{off} time. But an increase in pulsed current density at constant pulse charge and at constant T_{off} implies a decrease in grain-size. Therefore, a short T_{on} prevents grain growth and increases the nucleation rate [32].

The frequency of the pulse is the reciprocal of the total pulse duration consisting of T_{on} and T_{off}. The pulse length T_{on} and T_{off} time had significant effect on grain size. A higher pulse duration at lower pulse frequencies indicates enough time for the charging (*Ton*) and discharging (*Toff*) of the double layer [36–38]. In contrast, at a high pulse frequency the double layer does not have enough time for charging and discharging [39, 40]. Thus, lower frequencies cause bigger grains while higher frequencies results in a grain refinement of the electrodeposits [36–41, 84].

The deposition rate in the pulse technique is governed by the pulse current density (J_{peak}), and on time (T_{on}) and off time (T_{off}). At a given peak current density, the duty cycle is given by:

$$\text{Duty Cycle } (\%) = \frac{T_{on}}{T_{on} + T_{off}} \tag{17}$$

As discussed already, the average current density ($J_{average}$) in a pulse electrodeposition is given by:

$$J_{average} = \text{Duty Cycle} \times J_{peak} \tag{18}$$

where J_{peak} is the peak current density. A 100% duty cycle means there is no pulse used. The effect of pulse parameters has been studied in a paper by Sharma *et al*. [54], where they used various combinations of pulse on and on time to produce several duty cycles as shown in Table 2. These combinations are not unique and can be varied according to the desired changes in deposit microstructures.

Duty Cycle (%)	T_{on} **(s)**	T_{off} **(s)**
4	0.00042	0.01
10	0.0011	0.01
20	0.0025	0.01
40	0.0067	0.01
60	0.0150	0.01

(Reprinted "With kind permission from Springer Science+Business Media: Journal of Metallurgical and Materials Transactions A, Volume 45, 2014, Issue 10, Page 4610-4622, A. Sharma, S. Bhattacharya, S. Das, K. Das, Table II. © The Minerals, Metals & Materials Society and ASM International 2014").

Table 2. Pulse parameters at various duty cycles.

However, at a duty cycle of 100%, the grain size observed is usually much coarser. Thus, it is inferred that the grain size of the deposits decreases with an increase in *Ton* (at constant T_{off} and J_{peak}). An increase in *Ton* (longer current on times) results in an increased overpotential [84]. Youssef and his co-workers have also observed similar behavior in zinc electrodeposits [85]. It is reported that the deposit grain size decreases up to a duty cycle of 44%, and an increase in the grain size is noticed beyond duty cycle of 44%. This may be explained due to the fact that the pulse deposition gets transformed to the direct current deposition at this stage [85].

The pulse current (PC) with lower duty cycle (<20%) produces uniform and compact deposits. At higher duty cycles (>20%) and at direct current (DC) deposition, severe increase porosity is observed. This may be due to higher average current flow time *Ton*, which triggers hydrogen gas evolution [86]. This type of porous deposit morphology can be attributed to the dissolved hydrogen and oxygen gases in the plating bath. A higher solubility of hydrogen (1617 and 43.3

mg/L in water) compared to that of the oxygen in water (43.3 mg/L), at 25ºC and a 1 bar favors the dissolution of hydrogen gas and its incorporation over oxygen in the deposits [86]. Therefore, the morphology is rather porous and rough beyond a duty cycle of 20%.

A reduced porosity in case of PC deposition with lower duty cycles can be correlated to the two factors. (i) partial diffusion of the hydrogen and oxygen gas away from the substrate during off time (*Toff*) and hence a suppressed absorption of hydrogen gas in the deposit; (ii) the total amount of gas generated during the electrolysis of water in on time (*Ton*) is less compared to a continuous DC [54, 86]. Therefore, pulse current with lower duty cycle will result in a uniform and dense morphology as compared to high duty cycles or DC deposition.

The morphology of electrodeposits is also influenced by the pulse frequency in the electrodeposition. The pulse frequency parameters varied according to Sharma *et al*. [54] and are shown in Table 3. These combinations are also not unique like the duty cycle and can be varied to obtain the optimum deposit microstructures.

Frequency (*f*) of the pulse is described as follows:

$$f = \frac{1}{\left(T_{on} + T_{off}\right)} \tag{19}$$

Frequency	10 Hz		50 Hz		100 Hz		500 Hz	
Duty Cycle	T_{on}(s)	T_{off}(s)	T_{on}(s)	T_{off}(s)	T_{on}(s)	T_{off}(s)	T_{on}(s)	T_{off}(s)
10%	0.01	0.09	0.002	0.018	0.001	0.009	.0002	.0018

(Reprinted "With kind permission from Springer Science+Business Media: Journal of Metallurgical and Materials Transactions A, Volume 45, 2014, Issue 10, Page 4610-4622, A. Sharma, S. Bhattacharya, S. Das, K. Das, Table III. © The Minerals, Metals & Materials Society and ASM International 2014").

Table 3. Pulse frequency parameters

Lower pulse frequency (*f*) indicates a longer pulse period (T_{on}+T_{off}) at a constant duty cycle (D), as shown in Equation (19). The pulse duration is higher at lower frequencies providing sufficient time for the charging and discharging of the double layer.

The Sn atoms can migrate freely to the most stable position facilitating the grain growth. An increase in the pulse frequency shortens the pulse duration, i.e., both T_{on} and T_{off} are smaller as shown in Table 3. Shanthi *et al*. have noticed a severe grain refinement during pulse current plating of silver alloy with short pulse and high frequency [84]. As already discussed, at high pulse frequencies the charging an discharging action of double layer gets poor. These phenomena results in very thin diffusion layers that make the transportation of the migrating Sn ions towards cathode difficult. The nucleation rate improves as a consequence a dense microstructure is obtained [85, 66].

6.6. Effect of agitation

Agitation in the plating solution can be produced either by agitating the electrolyte or by moving the cathode. At low agitation rates, the effect of agitation on deposit composition is not visible, while the agitation rates may decrease the tin content in the coatings. Moreover, agitation may also increase the deposit roughness up to some extent [42, 54]. Agitation has beneficial effects of increasing the plating rate and permits the use of higher current densities by lowering polarization [36, 37, 38, 39]. Wen and Szpunar studied the nucleation and growth of tin and pointed out that agitation should not exceed beyond a certain limit where turbulent flow occurs that cause the difficulty of tin ions supply to the cathode even at high current densities [87]. Thus the cathode coverage is poor and the deposition rate decreases.

It is interesting to note that the stirring rate of the bath has a significant effect on the deposit morphology. The deposition parameters, except the stirring speed that controls the bath agitation, are kept constant. During still deposition, the cathode coverage is poor, and irregular and non-uniform deposits are obtained. This can be explained as when no agitation is provided, the depositing ions from the electrolyte get deposited preferentially on the cathode. Thus, a concentration gradient is established in the vicinity of electrolyte/cathode interface. The deposition is uneven at this stage and morphology is very poor. When the bath stirring is increased, the concentration gradient is decreased and deposition rate increases [87, 88]. Further stirring of the bath will cause fast transportation of metal ions towards cathode. At a sufficiently high stirring rates of the plating bath, the flow of the electrolyte will be turbulent and the metal ions may move away from the cathode vigorously and a lowering in the deposition rate is observed [88].

7. Sensitivity of the variables and grain size distribution

The electrodeposition parameters considered in this investigation include current density, concentration of the additive, duty cycle, frequency, pH, temperature, and agitation. The obtained results in this work indicate that the pulsed current electrodeposition can be an efficient method for the electrosynthesis of tin deposits. The surface morphology evolution depends on the electrodeposition parameter that tries to modify the overpotential, in a direct or indirect way. The current density is the most sensitive of all the plating parameters which affects the deposit morphology severely. The nucleation rate and grain growth can be significantly controlled by changing the duty cycle to lower values up 5 to 20%. At higher duty cycles, the porous deposits are produced.

Smaller pulse frequency gives large grained deposits. Thus, a combination of duty cycle and pulse frequency can be optimized for an ultrafine grained or an optimum grain morphology depending upon the application. The presence of additives in the plating bath improves the surface finish and morphology if it is added up to its optimum concentration. The current density is found to decrease with bath pH increase. The grain size decreases as pH value increases due to the increase in the cathodic polarization. It is also noteworthy point that powdery deposits are too developed at very high pH due to the precipitation of stannic

hydroxides. An increase in bath temperature is noticed to raise the grain size of the deposits. However, a decrease in the electrolyte conductivity and current efficiency is noted at elevated temperatures due to the precipitation of metal ions in the plating bath. Bath stirring improves the availability of metal ions towards cathode and thus the deposition rate is enhanced before the flow of electrolyte turns turbulent where the metal ions move away from the cathode. The grain size is also increased due to the decrease in overpotential with bath stirring rate

Author details

Ashutosh Sharma[1*], Siddhartha Das[2] and Karabi Das[2]

1 Department of Materials Science and Engineering, University of Seoul, Seoul, Korea

2 Department of Metallurgical and Materials Engineering, Indian Institute of Technology Kharagpur, Kharagpur, India

References

[1] Abtew M, Selvaduray, G. Lead Free Solders in Microelectronics. Materials Science and Engineering R. 2000;27:95-141.

[2] Suganuma, K. Lead Free Soldering in Electronics – Science, Technology and Environmental Impact. New York: Marcell Dekker Inc; 2004.

[3] Tu KN, Zeng K. Tin-Lead (SnPb) Solder Reaction in Flip Chip Technology. Materials Science and Engineering R. 2001;34:1-58.

[4] Tummala RR. Fundamentals of Microsystems Packaging. McGraw-Hill; 2000. p. 185-210.

[5] Liu JP, Guo F, Yan YF, Wang WB, Shi YW. Development of Creep-Resistant, Nano-sized Ag Particle-Reinforced Sn-Pb Composite Solders. Journal of Electronic Materials. 2004;33(9):958-963.

[6] Sobiech M, Teufel J, Welzel U, Mittemeijer EJ, Hugel W. Stress Relaxation Mechanisms of Sn and SnPb Coatings Electrodeposited on Cu: Avoidance of Whiskering. Journal of Electronic Materials. 2011;40:2300-2313.

[7] Coombs C. Coombs' Printed Circuits Handbook. USA: McGraw Hill; 2001. p. 45.1-45.9.

[8] Subramanian KN. Lead free electronic solders. A special issue of the Journal of Materials Science: Materials in Electronics. New York: Springer science; 2007. p. 55-76.

[9] Suganuma K. Advances in Lead-Free Electronics Soldering. Current Opinion in Solid State and Materials Science. 2001;5:55-64.

[10] Puttlitz KJ, Gaylon GT. Impact of RoHS Directive on High Performance Electronic Systems. Journal of Materials Science: Materials in electronics. 2007;18: 347-365.

[11] Gilleo K. Area Array Packaging Handbook. New York: McGraw-Hill; 2002.

[12] Puttiltz KJ, Stalter KA. Handbook of Solder Technology for Microelectronic Assemblies. New York: Marcell Dekker Inc; 2004. p. 51-55.

[13] Pecht M, Fukuda Y, Rajagopal S. The Impact of Lead-Free Legislation Exemptions on the Electronics Industry. IEEE Transactions on electronics packaging manufacturing. 2004;27:221-232.

[14] Plumbridge WJ. Tin Pest Issues in Lead-Free Electronic Solders. Journal of Materials Science: Materials in Electronics. 2007;18:307–318.

[15] Wang Y, Lu KH, Gupta V, Stiborek L, Shirley D, Im J, Ho PS. Effect of Sn Grain Structure on Electromigration Reliability of Pb-Free Solders. In: Proceedings of Electronic Components and Technology Conference; 2011. p. 711-716.

[16] Alam ME, Nai SML, Gupta M. Development of High Strength Sn–Cu Solder Using Copper Particles at Nanolength Scale. Journal of Alloys and Compounds. 2009;476:199-206.

[17] Shen J, Chan YC. Research Advances in Nano-Composite Solders. Microelectronics Reliability. 2009;49:223-234.

[18] Amagai M. A Study of Nanoparticles in Sn–Ag Based Lead Free Solders. Microelectronics Reliability. 2008;48:1-16.

[19] Chen Z, Shi Y, Xia Z, Yan Y. Properties of Lead-Free Solder SnAgCu Containing Minute Amounts of Rare Earth. Journal of Electronic materials. 2003;32(4):235-243.

[20] Brusse JA, Ewell GJ, Siplon JP. Tin Whiskers: Attributes And Mitigation. In: Proceedings of 16th Passive Components Symposium (CARTS EUROPE 2002); 2002. p. 221-233.

[21] Tu KN. Cu-Sn Interfacial Reactions: Thin-Film Case Versus Bulk Case, Materials Chemistry and Physics. 1996;46:217-223.

[22] Takenaka T, Kano S, Kajihara M, Kurokawa N, Sakamoto K. Growth Behavior of Compound Layers in Sn/Cu/Sn Diffusion Couples During Annealing at 433–473K. Materials Science and Engineering. 2005;396:115-123.

[23] Nakahara S, McCoy RJ, Buene L, Vandenberg JM. Room Temperature Interdiffusion Studies of Au/Sn Thin Film Couples. Thin solid films. 1981;84:185-196.

[24] Simic V, Marinkovic Z. Room Temperature Interactions in Copper Metal Thin Film Couples. Journal of less common metals. 1980;72:133-140.

[25] Tang WM, He A, Liu Q, Ivey DG. Solid State Interfacial Reactions in Electrodeposited Ni/Sn Couples. International Journal of Minerals, Metallurgy and Materials. 2010;17(4):459-463.

[26] Marinkovic Z, Simic V. Room Temperature Interactions in Ni/Metal Thin Film Couples. Thin solid films. 1982;98:95-100.

[27] Gaylon GT. Annotated Tin Whisker Bibliography. NEMI Tin Whisker Modeling Project; July 2003.

[28] Liangfeng L, Tai Q, Jian Y, Yongbao F. Synthesis of Ag-Cu-Sn Nanocrystalline Alloys as Intermediate Temperature Solder by High Energy Ball Milling. Advanced Materials Research. 2009;79-82:449-452.

[29] Hong Z, Ming TW, Qing XG, Cheng WY, Xiang ZZ. Synthesis of Sn–Ag Binary Alloy Powders by Mechanical Alloying. Materials Chemistry and Physics. 2010;122: 64-68.

[30] Aggarwal AO, Abothu IR, Raj PM, Sacks MD, Tummala RR. Lead-Free Solder Films Via Novel Solution Synthesis Routes. IEEE Transactions on Components and Packaging Technologies. 2007;30:486-493.

[31] Hao H, Tian J, Shi YW, Lei YP, Xia ZD. Properties of Sn3.8Ag0.7Cu Solder Alloy with Trace Rare Earth Element Y Additions. Journal of Electronic Materials. 2007; 36 (7): 766-774.

[32] Hsiao Li-Yin, Duh Jenq-Gong. Synthesis and Characterization of Lead Free Solders With Sn-3.5Ag-xCu (x = 0.2, 0.5, 1.0) Alloy Nanoparticles by the Chemical Reduction Method. Journal of Electrochemical Society. 2005;159(9):J102-J109.

[33] Conway PP, Fu EKY, Williams K. Precision High Temperature Lead-Free Solder Interconnections by Means of High-Energy Droplet Deposition Techniques. CIRP Annals–Manufacturing Technology. 2002;51:177-180.

[34] Hsiung CK, Chang CA, Tzeng ZH, Ho CS, Chien FL. Study on Sn-2.3Ag Electroplated Solder Bump Properties Fabricated by Different Plating and Reflow Conditions. In: Proceedings of 9th Electronics Packaging Technology Conference; 2007. p. 719-724.

[35] Ruythooren W, Attenborough K, Beerten S, Merken P, Fransaer J, Beyne E, Hoof CV, Boeck JD, Celis JP. Electrodeposition for the Synthesis of Microsystems. 2000;10:101-107.

[36] Paunovic M, Schlesinger M. Fundamentals of Electrochemical deposition. New Jersey: John wiley and Sons; 2006.

[37] Brown R. RF/Microwave Hybrids Basics. Materials and Processes. Dordrecht: Kluwer Academic Publishers; 2004. p. 169-171.

[38] Bard AJ, Faulkner LR. Electrochemical Methods: Fundamentals and Applications. New York: John Wiley & Sons; 2001.

[39] Kanani N. Electroplating: Basic Principles, Processes and Practice. Oxford: Elsevier Ltd; 2004.

[40] Chandrasekar MS, Pushpavanam M. Pulse and Pulses Reverse Plating-Conceptual, Advantages and Applications. Electrochimica Acta. 2008;53:3313-3322.

[41] Djokic SS. Modern Aspects of Electrochemistry-Electrodeposition Theory and Practice. New York: Springer; 2010.

[42] Tan AC. Tin and Solder Plating in the Semiconductor Industry. London: Chapman &. Hall; 1993.

[43] Schlesinger M, Paunovic M. Modern Electroplating. Hoboken, New Jersey: John wiley and sons; 2010.

[44] Abdel Rahim SS, Awad A, El Sayed A. Role of halides in the electroplating of tin from the alkaline stannate bath. Surface and coating Technology. 1986;28:139-150.

[45] Broggi RL, Oliviera GMD. Barbosa LL, Pallone EMJA, Carlos IA. Study of an Alkaline Bath for Tin Deposition in the Presence of Sorbitol and Physical and Morphological Characterization of Tin Film. Journal of Applied Electrochemistry. 2006;36:403-409.

[46] Sharma A, Bhattacharya S, Sen R, Reddy BSB, Fecht H-J, Das K, Das S. Influence of Current Density on Microstructure of Pulse Electrodeposited Tin Coatings. Materials Characterization. 2012;68:22-32.

[47] Lowenheim F A. Modern Electroplating. New York: John Wiley and Sons; 1974.

[48] Rehim SSAE, Refaey SA, Schwitzgebel G, Taha F, Saleh MB. Electrodeposition of Sn-Co Alloys From Gluconate Baths. Journal of applied electrochemistry. 1996;26:413-418.

[49] Tzeng GS, Lin SH, Wang YY, Wan CC. Effect of Additives on the Electrodeposition of Tin From an Acidic Sn(II) Bath. Journal of applied electrochemistry. 1996;26:419-423.

[50] Nakamura Y, Kaneko N, Nezu H. Surface Morphology and Crystal Orientation of Electrodeposited Tin From Acid Stannous Sulphate Solutions Containing Various Additives. Journal of applied electrochemistry. 1994;24:569-574.

[51] Fukuda M, Imayoshi K, Matsumoto Y. Effect of Adsorption of Polyoxyethylene Laurylether on Electrodeposition of Pb-free Sn Alloys. Surface and Coatings Technology. 2003;169-170:128-131.

[52] Medvedev GI, Makrushin NA. Electrodeposition of Tin From Sulfate Electrolyte With Organic Additives. Russian Journal of Applied Chemistry. 2001;74(11):1842-1845.

[53] He A, Liu Q, Ivey DG. Electrodeposition of Tin: A Simple Approach. Journal of Materials Science: Materials in Electronics. 2008;19:553-562.

[54] Sharma A, Bhattacharya S, Das S, Das K. A Study on the Effect of Pulse Electrodeposition Parameters on the Morphology of Pure Tin Coatings. Metallurgical and Materials Transactions A. 2013;45A:4610-4622.

[55] Gillman HD, Fernandes B, Wikiel K. Metal Alloy Sulfonic Acid Electroplating Baths. US Patent 6183 619 B1; Feb 6 2001.

[56] Sharma A, Bhattacharya S, Das S, Das K. Influence of current density on surface morphology and properties of pulse plated tin films from citrate electrolyte. Applied Surface Science. 2014;290:373-380.

[57] Martyak NM, Seefeldt R. Additive-Effects During Plating in Acid Tin Methanesulfonate Electrolytes. Electrochimica Acta. 2004;49:4303-4311.

[58] Low CTJ, Walsh FC. The Influence of a Perfluorinated Cationic Surfactant on the Electrodeposition of Tin from a Methanesulfonic Acid Bath. Journal of Electroanalytical Chemistry. 2008;615:91-102.

[59] Kim RH, Nam DH, Kwon HS. Electrochemical Performance of a Tin Electrodeposit With a Multi-Layered Structure for Li-ion Batteries. Journal of Power Sources. 2010;195:5067-5070.

[60] Vaid J, Char TLR. Tin Plating From the Pyrophosphate Bath. Journal of Electrochemical society. 1957;104(5):282-287.

[61] Harper CA. Electronic Materials and Processes Handbook. New York: McGraw-Hill; 2004.

[62] Ozga P. Electrodeposition of Sn-Ag and Sn-Ag-Cu Alloys From Thiourea Aqueous Solutions. Archives of Metallurgy and Materials. 2006;51:413-421.

[63] Fukuda M, Imayoshi K, Matsumoto Y. Effects of Thiourea and Polyoxyethylene Lauryl Ether on Electrodeposition of Sn-Ag-Cu Alloy as a Pb-Free Solder. Journal of Electrochemical Society. 2002;149:C244-C249.

[64] Lin KL, Sun LM. Electrodeposition of eutectic Sn–Zn alloy by pulse plating. Journal of Materials Research. 2003;18:2203-2207.

[65] Lačnjevac U, Jović BM, Jović VD. Electrodeposition of Ni, Sn and Ni–Sn Alloy Coatings from Pyrophosphate-Glycine Bath. Journal of Electrochemical Society. 2012;159(5):D310-D318.

[66] Ibl N. Some Theoretical Aspects of Pulse Electrolysis. Surface Technology. 1980;10:81-104.

[67] Watanabe T. Nano-Plating Microstructure Control Theory of Plated Film and Data Base of Plated Film Microstructure. Oxford UK: Elsevier Ltd; 2004.

[68] Sharma A, Bhattacharya S, Das S, Das K. Fabrication of Sn-Ag/CeO2 Electro-Composite Solder by Pulse Electrodeposition. Metallurgical and Materials Transactions A. 2013;44A:5587-5601.

[69] Liu Z, Zheng M, Hilty RD, West AC. Effect of Morphology and Hydrogen Evolution on Porosity of Electroplated Cobalt Hard Gold. Journal of Electrochemical Society. 2010;157 (7):D411-D416.

[70] Nikolic ND, Popov KI, Pavlovic LJ, Pavlovic MG. Morphologies of Copper Deposits Obtained by the Electrodeposition at High Overpotentials. Surface and Coatings Technology. 2006;201:560-566.

[71] Durney LJ. Electroplating Engineering Handbook. 4th ed. London: Chapman & Hall; 1984.

[72] Teshigawara T, Nakata T, Inoue K, Watanabe T. Microstructure of Pure Tin Electrodeposited Films, Scripta Materialia. 2001;44:2285-2289.

[73] Ebrahimi F, Bourne GR, Kelly MS, Matthews TE. Mechanical Properties of Nanocrystalline Nickel Produced by Electrodeposition. Nanostructured Materials. 2009;11(3): 343-350.

[74] Natter H, Hempelmann R. Nanocrystalline Copper by Pulsed Electrodeposition: The Effects of Organic Additives, Bath Temperature, and pH. Journal of Physical Chemistry. 1996;100:19525-19532.

[75] Sahaym U, Miller SL, Norton MG. Effect of Plating Temperature on Sn Surface Morphology. Materials Letters. 2010;64:1547-1550.

[76] Lee JY, Kim JW, Chang BY, Kim HT, Park SM. Effects of Ethoxylated α-Naphtholsulfonic Acid on Tin Electroplating at Iron Electrodes. Journal of The Electrochemical Society. 2004;151(5):C333-C341.

[77] Aragon A, Figueroa MG, Gana RE, Zagal JH. Effect of Polyethoxylate Surfactant on the Electrodeposition of Tin. Journal of Applied Electrochemistry. 1992;22: 558-562.

[78] Lal S, Moyer TD. Role of Intrinsic Stresses in the Phenomena of Tin Whiskers in Electrical Connectors. IEEE Transactions on Electronics Packaging Manufacturing. 2005;28:63-74.

[79] Song JY, Yu J, Lee TY. Effects of Reactive Diffusion on Stress Evolution in Cu–Sn Films. Scripta Materialia. 2004;51:167-170.

[80] Sekar R, Eagammai C, Jayakrishnan S. Effect of Additives on Electrodeposition of Tin and its Structural and Corrosion Behaviour. Journal of Applied Electrochemistry. 2010;40:49-57.

[81] Neveu B, Lallemand F, Poupon G. Mekhalif Z. Electrodeposition of Pb-free Sn alloys in pulsed current. Applied Surface Science. 2006;252:3561-3573.

[82] Correia AN, Facanha MX, Lima-Neto P. de Cu–Sn Coatings Obtained From Pyrophosphate-Based Electrolytes. Surface and Coatings Technology. 2007;201:7216- 7221.

[83] Franklin TC. Some Mechanisms of Action of Additives in Electrodeposition Processes. Surface and Coatings Technology. 1987;30:415-428.

[84] Shanthi C, Barathan S, Jaiswal R, Arunachalam RM, Mohan S. The Effect of Pulse Parameters in Electrodeposition of Silver Alloy. Materials Letters. 2008;62:4519- 4521.

[85] Youssef Kh MS, Koch CC, Fedkiw PS. Influence of Additives and Pulse Electrodeposition Parameters on Production of Nanocrystalline Zinc from Zinc Chloride Electrolytes. Journal of Electrochemical Society. 2004;151(2):C103-C111.

[86] Besra L, Uchikoshi T, Suzuki TS, Sakka Y. Application of Constant Current Pulse to Suppress Bubble Incorporation and Control Deposit Morphology During Aqueous Electrophoretic Deposition (EPD). Journal of the European Ceramic Society.

[87] 2009;29:1837-1845.

[88] Wen S, Szpunar JA. Nucleation and Growth of Tin on Low Carbon Steel. Electrochimica Acta. 2005;50:2393-2399.

[89] Musa AY, Slaiman QJM, Kadhum AAH, Takriff MS. Effects of Agitation, Current Density and Cyanide Concentration on Cu-Zn Alloy Electroplating. European Journal of Scientific Research. 2008;22(4):517-524.

IntechOpen